International Journal of Ambient Energy, 2015
http://dx.doi.org/10.1080/01430750.2015.1023466

Taylor & Francis
Taylor & Francis Group

Artificial neural network-based prediction of performance and emission characteristics of CI engine using polanga as a biodiesel

Abhishek Sharma[a*], Pradeepta Kumar Sahoo[b], R.K. Tripathi[b] and Lekha Charan Meher[c]

[a]*Department of Mechanical Engineering, Ideal Institute of Technology, Ghaziabad 201002, India;* [b]*Department of Mechanical Engineering, College of Engineering Studies, UPES, Dehradoon, India;* [c]*DRDO, Secundrabad, India*

(*Received 16 September 2014; accepted 23 February 2015*)

The present work predicts the performance parameters, namely brake specific fuel consumption (BSFC), brake thermal efficiency (BTE), peak pressure, exhaust gas temperature and exhaust emissions of a single cylinder four-stroke diesel engine at different injection timings and engine load using blended mixture of polanga biodiesel by artificial neural network (ANN). The properties of biodiesel produced from polanga were measured based on ASTM standards. Using some of the experimental data for training, an ANN model was developed based on standard back-propagation algorithm for the engine. Multi-layer perception network was used for non-linear mapping between input and output parameters. Different activation functions and several rules were used to assess the percentage error between the desired and the predicted values. It was observed that the developed ANN model can predict the engine performance and exhaust emissions quite well with correlation coefficient (R) 0.99946, 0.99968, 0.99988, 0.99967, 0.99899, 0.99941 and 0.99991 for the BSFC, BTE, peak pressure, exhaust gas temperature, NO_x, smoke and unburned hydrocarbon emissions, respectively. The experimental results revealed that the blended fuel provides better engine performance and improved emission characteristics.

Keywords: biodiesel; ANN; performance; emission; compression ignition (CI) engine; diesel engine

1. Introduction

Rapidly increasing energy demand of the world due to modernisation and industrialisation has led to a large number of developing countries importing crude oil other than indigenous production to cope up their increasing energy demand. Thus, a major chunk of their export earnings is spent on purchase of petroleum products. Besides the fuel crisis, the other problem of concern is the degradation of environment due to fossil fuel combustion. Thus it is essential that low emission alternate fuels must be developed for use in diesel engines. Biodiesel has been widely recognised in the alternative fuel industry (Ghobadian et al. 2009). The attractive features of biodiesel fuel are (i) it is plant-derived, and as such its combustion does not increase current net atmospheric levels of greenhouse gas; (ii) it can be domestically produced, offering the possibility of reducing petroleum imports; (iii) it is biodegradable and (iv) relative to conventional diesel fuel, its combustion products have reduced levels of particulates, carbon monoxide and, in some conditions, nitrogen oxides. The research and development activities on biodiesel have been mostly on sunflowers, saffola, soyabean, rapeseed and peanut which are considered edible in several countries (Sahoo et al. 2007; Baiju, Naik, and Das 2009). However, biodiesel can also be produced from non-edible oil seeds like jatropha, karanja, neem, cotton, rubber, polanga, etc. (Ramadhas, Jayaraj, and Muraleedharan 2005). Sahoo et al. (2007) conducted engine tests using polanga-based biodiesel and recommended its use as an alternative fuel for the existing conventional diesel engines without any major hardware modifications. The density and viscosity of the polanga oil methyl ester formed after triple stage transesterification were found to be close to those of petroleum diesel oil. Sahoo et al. (2009) evaluated comparative performance and emission characteristics of jatropha-, karanja- and polanga-based biodiesel as fuel in a tractor engine. They observed that brake specific fuel consumption (BSFC) for all the biodiesel blends with diesel increased with blends and decreased with speed. The study however lacks the effect of advancing or retarding the injection timing on engine performance. Injection timing along with blend percentage is also an important parameter that may affect the performance and emission characteristics (Shivakumar, Srinivasa Pai, and Shrinivasa Rao 2011).

The performance of a CI engine for various proportions of blends, for various compression ratios and at different injection timings and pressures are usually desired by engine manufacturers and engineers. This can be obtained either by conducting comprehensive tests or by modelling the engine operation. Testing the engine under all possible

*Corresponding author. Email: absk2001@gmail.com

operating conditions and fuel cases are both time consuming and expensive. On the other hand developing an accurate model for the operation of a CI engine fuelled with blends of biodiesel is too difficult due to the complex nature of the processes involved. So, as an alternative, engine performance and exhaust emissions can be modelled using artificial neural networks (ANNs). ANN can be used to solve a wide variety of problems in science and engineering, particularly in some areas where the conventional modelling methods fail. The predictive ability of an ANN results from the training on experimental data and then validation by independent data. An ANN model can accommodate multiple input variables to predict multiple output variables. The prediction by a well-trained ANN is normally much faster than the conventional simulation programmes or mathematical models as no lengthy iterative calculations are needed to solve differential equations using numerical methods but the selection of an appropriate neural network topology is important in terms of model accuracy and model simplicity. In addition, it is possible to add or remove input and output variables in the ANN if it is needed. Canakci and Gerpen (2003) investigated the engine performance and emissions characteristics of two different petroleum diesel-fuels (No. 1 and No. 2), biodiesels (from soybean oil and yellow grease) using ANNs where 20% blends with No. 2 diesel fuel were used as experimental results. In this study, the average molecular weight, net heat of combustion, specific gravity, kinematic viscosity, C/H ratio and cetane number of each fuel were used as the input layer, while outputs were the BSFC, exhaust temperature and exhaust emissions. The back-propagation learning algorithm with three different variants, single layer and logistic sigmoid transfer function were used in the network. The network yielded R^2 values of 0.99 for both training and test data. The mean % errors were smaller than 4.2 and 5.5 for the training and test data, respectively. Ghobadian et al. (2009) developed an ANN model of a diesel engine using waste cooking biodiesel fuel with standard back-propagation algorithm. The developed model predicted the engine performance and exhaust emissions quite well with correlation coefficient (R) 0.9487, 0.999, 0.929 and 0.999 for the engine torque, specific fuel consumption (SFC), carbon monoxide (CO) and hydrocarbon (HC) emissions, respectively. The predicted mean square error (MSE) was between the desired outputs as measured values and the simulated values were obtained as 0.0004 by the model. Canakci et al. (2009) used ANN to model performance parameters and emissions of a biodiesel engine using waste cooking oil. Engine speed and percentage of blend were taken as the input variables and brake power, torque, SFC and exhaust emissions as the outputs. It was observed that the regression values for most of the parameters were close to unity. Yusaf et al. (2010) conducted experiments in a diesel engine fuelled with a combination of both compressed natural gas and diesel fuel. ANN modelling was used to predict brake power, torque, BSFC and engine emissions. A good correlation between predicted and the experimental values was observed. Ismail et al. (2012) reported an ANN model programmed for a light-duty diesel engine. Engine operating parameters, namely engine speed, output torque, fuel mass flow rate and biodiesel fuel types and blends were used as the input parameters in the model. The results indicated that back-propagation feed-forward neural network, combination of tansig/purelin transfer functions, trainlm training algorithm were the optimum configuration to predict the correlations. Çay et al. (2013) used ANN modelling to predict the BSFC, effective power and average effective pressure and exhaust gas temperature of the methanol engine. It was found that the R^2 values were close to 1 for both training and testing data. Root mean square (RMS) values were smaller than 0.015 and mean errors were smaller than 3.8% for the testing data. Ahmadi et al. (2013a) proposed a model based on a feed-forward ANN optimised by hybrid genetic algorithm particle swarm optimisation (HGAPSO) to estimate the power of the solar stirling heat engine. Particle swarm optimisation (PSO) was used to decide the initial weights of the neural network. The results demonstrated the effectiveness of the HGAPSO-ANN model. Ahmadi et al. (2013b) investigated the optimal power of an endoreversible Stirling cycle with perfect regeneration. Optimal temperature of the heat source leading to a maximum power for the cycle was detained. Moreover, effect of design parameters of the Stirling engine on the maximised power of the engine and its corresponding thermal efficiency was studied. Ahmadi et al. (2013) investigated thermodynamic analysis and non-dominated sorting genetic algorithm (NSGA)-II algorithm were employed to optimise objective function associated to the power output, thermal efficiency for a solar-driven engine system. Three decision-making procedures were applied to optimised answers from the results. The error through investigation was shown using error analysis. Ahmadi et al. (2013c) optimised output power and engine thermal efficiency and total pressure losses were minimised using NSGA algorithm and finite speed thermodynamic analysis. The results were successfully verified against experimental data. Ahmadi et al. (2014a) implemented ANN to estimate the torque of the Stirling heat engine. In addition, highly accurate actual values of the required parameters which were gained from open literature surveys from previous studies were implemented to develop a robust intelligent model. Based on the outcomes of the ANN approach, the output results of an ANN model were close to relevant actual values with a high degree of performance. Ahmadi et al. (2014b) employed multi-objective evolutionary algorithms based on the NSGA-II algorithm, while effectiveness of the regenerator, effectiveness of low- and high-temperature heat exchangers, effectiveness of high-temperature heat exchanger, temperatures of the hot side and cold side, and dead volume ratio were considered as decision variables. After the definition of the

Pareto optimal frontier, the final optimal solution was selected using different decision-making methods such as the fuzzy Bellman–Zadeh, linear programming technique for multidimensional analysis of preference (LINMAP) and technique for order of preference by similarity to ideal solution (TOPSIS). Toghyani, Kasaeian, and Ahmadi (2014), optimised the efficiency and the power loss due to pressure drop into the heat exchangers for a Stirling system using non-ideal adiabatic analysis and the second-version nondominated sorting genetic algorithm. The optimised answers were chosen from the results using three decision-making methods. The applied methods were compared at last and the best results were obtained for the technique for order preference by similarity to ideal solution decision-making method. Toghyani et al. (2015) applied ANN to estimate the power and torque values obtained from a Stirling heat engine. It employed the Levenberg–Marquardt algorithm for training ANN with back-propagation network for estimating the power and torque of the Stirling heat engine. Considering the results obtained from this study, there was very good agreement between the output of the testing phase of the ANN-PSO model with experimental data. In the present work, experimental investigations of the performance and emissions of the diesel engine were conducted for different proportions of blends of polanga with diesel at different injection timings and for different loads. Using data from experimental results, ANN models have been developed for the performance parameters and emissions characteristics. In the model, blends of polanga with diesel, different injection timings and loads are taken as input parameters and BSFC, brake thermal efficiency (BTE), peak pressure, exhaust gas temperature, NO_x, smoke and HC emissions are taken as output parameters. The application of ANN for modelling for both the performance parameters and emission characteristics is an effort to comprehensively understand the modelling capability of ANN, which will really help in better prediction with the available experimental data.

2. Experimental investigation

The engine used in the present study was a Kirloskar make single cylinder four-stroke water cooled CI engine. The detailed specification of the engine is shown in Table 1. The schematic diagram of the experimental set-up is shown in Figure 1. The experimental set-up consists of engine, dynamometer, load cell, temperature sensors, etc. Eddy current-dynamometer was used for engine loading. A fuel consumption meter, differential pressure (DP) transmitter, range 0–500 mm wc, was used for measuring the SFCs of the engine. A Kistler make quartz (piezo-electric) transducer in conjunction with a Kistler charge amplifier was employed to determine the cylinder gas pressure. The pressure transducer had range up to 345 bar. Real-time data acquisition was done with the help of Engine Test Express V5.76 which was Labview-based software package. Exhaust gas analyzer of AVL make (AVL DiGas 444) was used for measuring the emissions of HC, and NO_x from the engine. A smoke meter, model 437C, made by AVL Gurgaon, was used for measuring the smoke emission from engine. Exhaust gas emissions recorded were unburned hydrocarbons (UBHC) in parts per million (ppm) and oxides of nitrogen (NO_x) in ppm by using gas analyzer. Opacity of the smoke in the exhaust was measured in % by using smoke meter. K-type thermocouples were employed to assess the exhaust gas, cooling water inlet and outlet temperatures.

Table 1. Engine specifications.

Item description	Kirloskar
Brake horse power (BHP)	5HP
Speed	1500
Number of cylinders	1
Compression ration	16.7:1
Bore	80 mm
Stroke	110 mm
Orifice diameter	20 mm
Type of ignition	Compression ignition
Method of loading	Eddy current dyanometer
Method of starting	Manual cranking
Method of cooling	Water

The performance test of the engine included fuel consumption and rating test. In order to carry out fuel consumption test, initially the engine was started and warmed up on zero loads. After that the engine was gradually loaded up to 100% load to stabilise its operation. The fuel consumption test of the engine on different fuels was then carried out at the selected loads. The experiment with each selected fuel type was replicated three times and the average value of different performance and emission parameters measured was taken for analysis. In the present investigation, biodiesel derived from polanga oil was used as the test fuel. Biodiesel preparation through transesterification process has already been reported in previous studies (Sahoo et al. 2007, 2009). Four biodiesel blends of polanga were used, namely BD10, BD20, BD30 and BD40. The physical and chemical properties of biodiesel were determined as per ASTM standard test methods. The injection timing of the engine was kept at 23° before top dead center (bTDC) (as set by the manufacturer) initially and the fuel was altered to biodiesel. By keeping injection timing at 23° bTDC, the load was differed from 20% to 100% in the interval of 20%. The observations were taken at brake power of 0.7, 1.5, 2.2, 2.9 and 3.7 kW. The performance, emissions and combustion characteristics of diesel engine were recorded for BD20 with a constant speed of 1500 rpm. Similar procedures were repeated for other biodiesel blends at the same injection timings. To visualise the effect of injection timing, the entire procedure was repeated for injection timings of 15°, 19°, 27° and 31° bTDC.

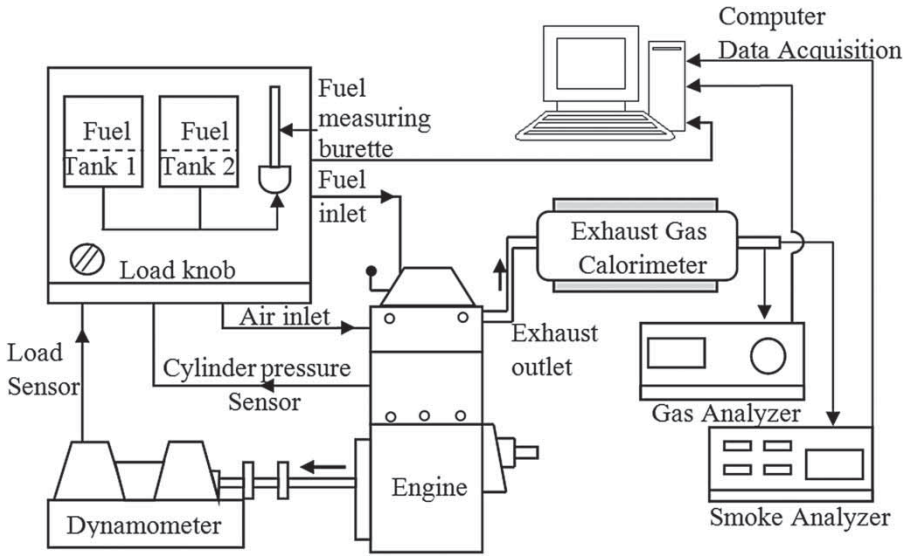

Figure 1. Experimental set-up.

3. Neural network design

3.1. *Artificial neural networks*

ANNs are logic programming technique developed by imitating the operation of the human brain to perform functions such as learning, remembering, deciding and inference, without receiving any aid. ANNs have various important features, such as learning from data, generalisation, working with an infinite number of variables, etc. Artificial neural cells are the smallest units that form the basis of the operation of ANNs just like a biological neuron which receives inputs from other sources, combines them in some way, performs generally a non-linear operation on the result, and then outputs the final result. The artificial neural cells consist of mainly five elements, namely inputs, weights, summation functions, activation functions and outputs (Figure 2).

ANN has three main layers, namely the input, hidden and output layers. The inputs are data from the external source. The processing elements, called neurons, in the input layer transfers data from the external source to the hidden layer. The weights are the values of connections between cells. The outputs are produced using data from neurons in the input and hidden layers, and the bias, summation and activation functions. In the output layer, the output of network is produced by processing data from hidden layer and sent to external source. The summation function is a function which calculates the net input of the cell. The summation function used in this study is given in Equation (1)

$$\mathrm{NT}_i = \sum_{j=1}^{n} w_{ij} x_j + w_{bi}. \tag{1}$$

The activation function provides a curvilinear relation between the input and output layers. It also determines the output of the cell by processing the net input to the cell. The selection of an appropriate activation function significantly affects network performance. Commonly used activation

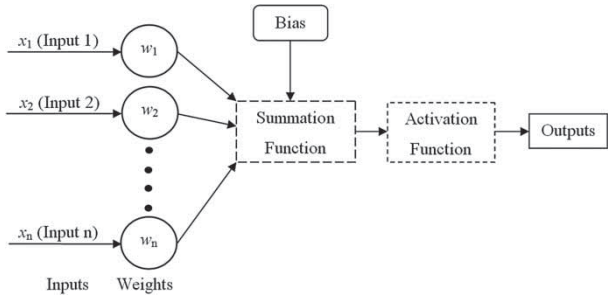

Figure 2. Structure of an artificial neural cell.

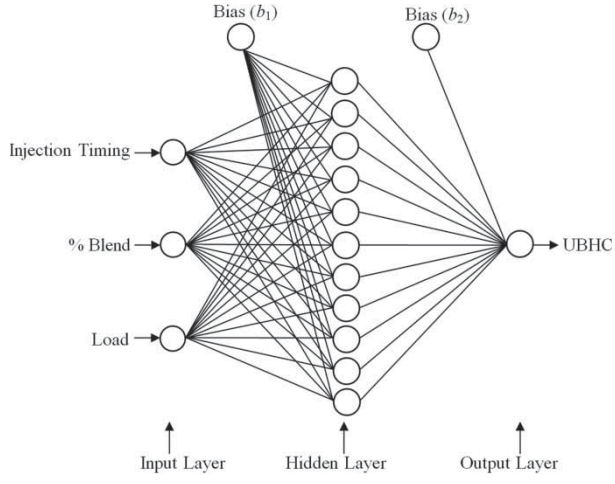

Figure 3. Best ANN architecture built for the prediction of UBHC.

Table 2. Correlation coefficients for outputs using different learning algorithms.

Parameter	Learning algorithm	Activation function	Neurons	Correlation coefficient (R)	
				Training	Testing
BTE	Trainlm	Sig/lin	5	0.99406	0.99004
	Trainlm	Sig/lin	6	0.99591	0.99081
	Trainlm	Sig/lin	10	0.99647	0.99221
	Trainlm	Sig/lin	15	0.99604	0.99694
	Trainlm	Sig/lin	20	0.99968	0.99651
	Trainlm	Tan/lin	10	0.9943	0.99067
	Trainscg	Sig/lin	5	0.9834	0.98096
	Trainscg	Sig/lin	6	0.98099	0.98137
	Trainscg	Sig/lin	10	0.98921	0.9853
	Traingdm	Sig/lin	10	0.8377	0.855
BSFC	Trainlm	Sig/lin	5	0.99358	0.99471
	Trainlm	Sig/lin	6	0.99709	0.98604
	Trainlm	Sig/lin	10	0.99727	0.99168
	Trainlm	Sig/lin	15	0.99881	0.99618
	Trainlm	Sig/lin	20	0.99946	0.99359
	Trainscg	Sig/lin	5	0.97973	0.98542
	Trainscg	Sig/lin	6	0.98729	0.9905
	Trainscg	Sig/lin	10	0.99007	0.97519
	Traingdm	Sig/lin	10	0.75024	0.81653
T_{ex}	Trainlm	Sig/lin	5	0.99819	0.99646
	Trainlm	Sig/lin	6	0.99898	0.99618
	Trainlm	Sig/lin	10	0.99931	0.99849
	Trainlm	Sig/lin	15	0.99967	0.99919
	Trainscg	Sig/lin	5	0.99397	0.99597
	Trainscg	Sig/lin	6	0.99321	0.99427
	Trainscg	Sig/lin	10	0.98791	0.99083
P_{max}	Trainlm	Sig/lin	5	0.99424	0.99404
	Trainlm	Sig/lin	6	0.9947	0.99633
	Trainlm	Sig/lin	10	0.99264	0.99384
	Trainlm	Sig/lin	20	0.99988	0.99587
	Trainscg	Sig/lin	5	0.97638	0.96727
	Trainscg	Sig/lin	6	0.98404	0.97345
	Trainscg	Sig/lin	10	0.97305	0.98589
NO_x	Trainlm	Sig/lin	5	0.99403	0.9852
	Trainlm	Sig/lin	6	0.99747	0.99329
	Trainlm	Sig/lin	10	0.99838	0.99327
	Trainlm	Sig/lin	15	0.99899	0.99659
	Trainlm	Sig/lin	20	0.99987	0.99873
	Trainlm	Tan/lin	10	0.9983	0.99396
	Trainscg	Sig/lin	5	0.98684	0.99406
	Trainscg	Sig/lin	6	0.98158	0.97792
	Trainscg	Sig/lin	10	0.98309	0.99188
	Traingdm	Sig/lin	10	0.93193	0.89309
Smoke	Trainlm	Sig/lin	5	0.98721	0.94474
	Trainlm	Sig/lin	6	0.98339	0.98946
	Trainlm	Sig/lin	10	0.99401	0.98814
	Trainlm	Sig/lin	15	0.99941	0.99628
	Trainlm	Sig/lin	20	0.99979	0.9956
	Trainlm	Sig/lin	25	0.99969	0.98134
	Trainlm	Tan/lin	10	0.99868	0.99375
	Trainscg	Sig/lin	5	0.95591	0.96122
	Trainscg	Sig/lin	6	0.96305	0.98925
	Trainscg	Sig/lin	10	0.98058	0.9458
	Traingdm	Sig/lin	10	0.92551	0.92046
UBHC	Trainlm	Sig/lin	5	0.97969	0.96352
	Trainlm	Sig/lin	10	0.99976	0.99905
	Trainlm	Sig/lin	11	0.99991	0.9998

functions are the threshold function, step activation function, sigmoid function and hyperbolic tangent function. The type of activation function depends on the type of neural network to be designed. A sigmoid function is widely used for the transfer function. Logistic transfer function of the ANN model in this study is given in Equation (2)

$$f(\mathrm{NT}_i) = \frac{1}{1 + e^{-\mathrm{NT}_i}}. \quad (2)$$

The significant advantages of ANNs are learning ability and the use of different learning algorithms. The most important factor which determines its success in practice, after the selection of ANN architecture, is the learning algorithm. In order to obtain the output values closest to the numerical values, the best learning algorithm and the number of optimum neurons in the hidden layer must be determined.

A most sought-after algorithm is the back-propagation algorithm, which has different variants. Back-propagation training algorithms such as conjugate gradient, quasi-Newton and Levenberg–Marquardt (LM) use standard numerical optimisation techniques. ANN with back-propagation algorithm learns by changing the weights which are stored as knowledge. The algorithm uses the second-order derivatives of the cost function so that a better convergence behaviour can be obtained. To get the best prediction by the network, several architectures were evaluated and trained using the experimental data. The back-propagation algorithm was utilised in training of all ANN models. In the training stage, to obtain the output precisely, the number of neurons in the hidden layer was increased step by step (i.e. 5–20). For this purpose, BFGS (quasi-Newton back-propagation), LM learning algorithm and scaled conjugate gradient (SCG learning algorithm) learning algorithms were used in the building of the network structure. As a result of conducted trials, the best learning algorithms for most of the parameters was found to be the LM learning algorithm. The best network structures for BTE, BSFC, T_{ex}, P_{max}, NO_x, smoke and UBHC were found to be 3-15-1, 3-15-1, 3-15-1, 3-20-1, 3-20-1, 3-15-1 and 3-11-1, respectively (Table 2). The best ANN architecture built for prediction of UBHC is shown in Figure 3. Also, correlation coefficients of BTE, BSFC, T_{ex}, P_{max}, NO_x, smoke and UBHC for different learning algorithms are given in Table 2.

In this study, 100 experimental data sets were prepared for the training and testing data for the ANN. The ratio for training and testing data was selected as 80%:20%, i.e. 20 and 80 sets of the experimental data were randomly selected for the testing data and training data, respectively. In the back-propagation model, the scaling of inputs and outputs dramatically affects the performance of an ANN. As mentioned above, the logistic sigmoid transfer function was used in this study. One of the characteristics of this function was that only a value between 0 and 1 can be produced. The input and output data sets were normalised between 0.1 and 0.9 before the training and testing process to obtain the optimal predictions. Linear function suited best for the output layer. This arrangement of functions in function approximation problems or modelling is common and yields better results. However many other networks with several functions and topologies were examined. Three criteria were used to evaluate the networks and find the optimum one among them. The training and testing performance (MSE) were chosen to be 0.00001 for all ANNs. The smaller ANNs had the priority to be selected as the complexity and size of the network was also important. Finally, a regression analysis between the network response and the corresponding targets was performed to investigate the network response in more detail. Different training algorithms were also tested and finally Levenberg–Marquardt (Trainlm) was selected. Neural network toolbox was used for ANN design.

4. Results and discussion

4.1. Biodiesel fuel characteristics and properties

Biodiesel is produced by the three stage transesterification process. The first stage removes the organic matters and other impurities present in the unrefined filtered polanga oil using reagent. The second stage reduces the acid value of the oil about 4 mg KOH/g corresponding to a free fatty acid (FFA) level of 2%. The product of the second stage (pure triglycerides) is transesterified to mono-esters of fatty acids (biodiesel) using alkali catalyst. It was observed that the biodiesel produced from polanga oil by above three stages, has the physico-chemical properties close to those of diesel. Fuel properties are mentioned in Table 3.

Table 3. Properties of polanga biodiesel and its blends.

Fuel	Calorific value (kJ/kg)	Viscosity (cSt)	Density (g/cc)	Flash point (°C)	Cloud point (°C)	Pour point (°C)
Diesel	43,996.3	2.91	0.830	77	6.4	− 4
10%B	40,094.2	3.1	0.839	82	7.2	2.8
20%B	39,193.73	3.2	0.847	88	7.9	3.1
30%B	38,393.3	3.32	0.855	94	8.2	3
40%B	37,792.98	3.6	0.863	99	8.6	3.2
Biodiesel	36,992.56	6.8	0.941	152	14.1	4.7

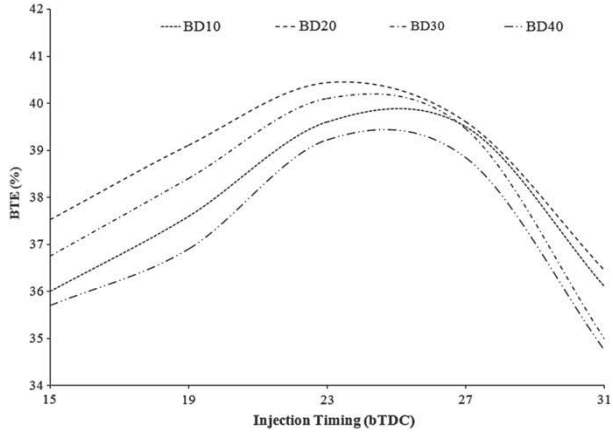

Figure 4. Variation of BTE with injection timings.

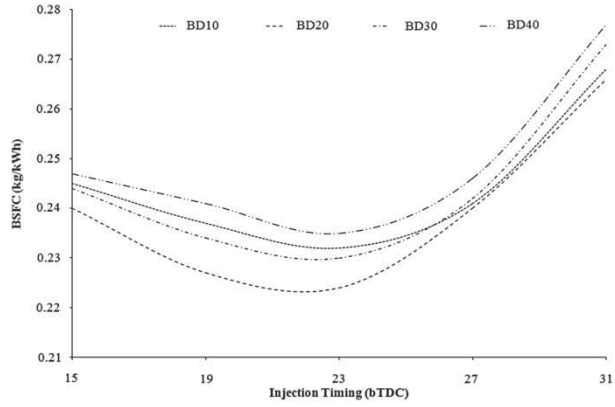

Figure 5. Variation of BSFC at different injection timings for different blends.

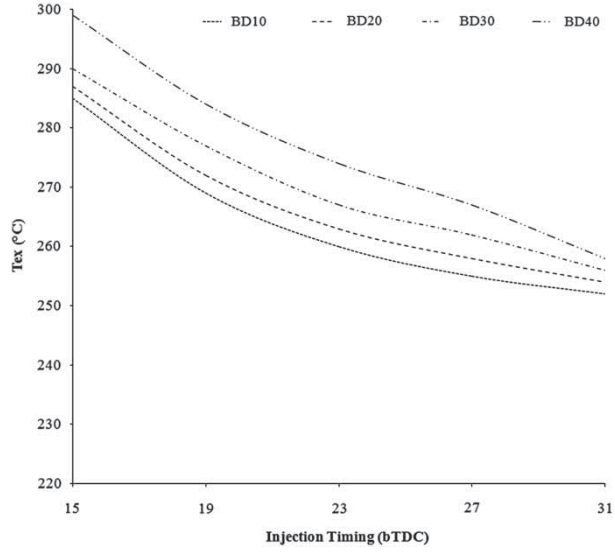

Figure 6. Variation of exhaust gas temperature (T_{ex}) with injection timing at full load.

4.2. Performance parameters

4.2.1. Brake thermal efficiency

Figure 4 shows the variation of BTE with injection timings at full load. As can be seen from Figure 4, BD20 shows higher values of brake thermal efficiencies on all the injection timings. When the injection was advanced by 4° from the normal injection timing (23° bTDC) there was reduction in the thermal efficiency by 1.33% for BD20. A further advance in injection by 4° resulted in reduction in thermal efficiency by 1.6%. This may be attributed to the increase in the delay period with the increase in injection advance angle. On the other hand for retarded injection timings the thermal efficiency at full load for B20 reduced by 3.0%. At retarded injection timings the delay period decreases which reduces the power because larger amount of fuel burns during expansion. Hence normal injection timing (23° bTDC) can be considered to be the best injection timing.

4.2.2. Brake specific fuel consumption

Figure 5 shows the BSFC at full load at different injection timings for different blends which shows that BSFC is minimum for all the blends at the best injection timing (23° bTDC) where as both for advanced as well as retarded values the brake specific energy consumption (BSEC) increases as is evident that thermal efficiency is maximum at this injection timing.

4.2.3. Exhaust gas temperature

The variation of exhaust gas temperature (T_{ex}) with the injection timing at full load for biodiesel blends is shown in Figure 6. The exhaust gas temperature is minimum for advanced injection timing for diesel and polanga blends. Advancing the injection timing caused earlier start of combustion relative to top dead center (TDC) and hence complete combustion will take place and thus reducing the exhaust gas temperatures. Of all the blends, BD10 shows lower values of exhaust gas temperature at all the injection timings.

4.3. Exhaust emissions

4.3.1. NO_x emission

One of the most critical emissions from the CI engines is NO_x emission. The formation of NO_x is highly dependent on cylinder temperature, oxygen concentration and residence time for the reaction to take place. Figure 7 shows the variation of NO_x with injection timings at full load condition. For the retarded injection timings NO_x emissions were found to be less whereas for advanced injection timings it increased. When the injection timing was advanced by 4° crank angle, the operating temperature increased and hence 5.4% increase in NO_x emission for BD20 at full load condition. An increase in blend percentage improves the NO_x emissions, BD40 shows lowest NO_x emissions. A further advance in injection by 4° results in sharp increase in NO_x emissions for all the blends. On the other hand when it was retarded by 4° crank angle, cylinder pressure and temperature decreased, since more fuel burns after TDC and thus sharply reducing NO_x emissions for all the

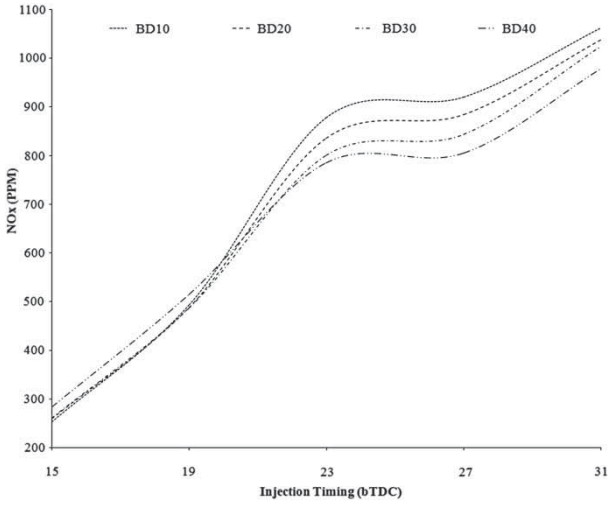

Figure 7. Variation of NO_x with injection timing for different blends at full load.

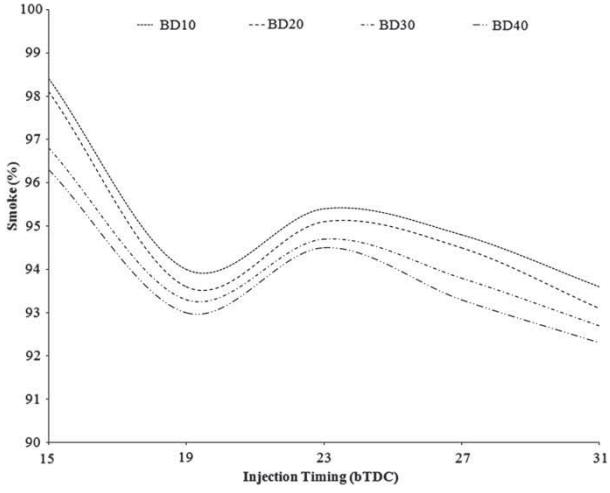

Figure 8. Variation of smoke emission with injection timings.

blends. BD40 shows the lowest NO_x emissions for advance injection timings under present study.

4.3.2. *Smoke emission*

Smoke formation occurs at extreme air deficiency. Air or oxygen deficiency is locally present inside the diesel engine. It increases as the air–fuel ratio decreases. Experimental results indicate that smoke emissions decrease with blending of diesel. Figure 8 shows the variation of smoke emission with injection timings for all the blends. It is very clear from the graph that for advanced injection timings, the smoke emissions were reduced since cylinder operating temperatures were higher at advanced injection timing. Because of higher temperature and pressure there is an improved reaction between fuel and oxygen, and thus reduces the smoke. BD40 shows the lowest smoke emissions for all the injection timings under present study.

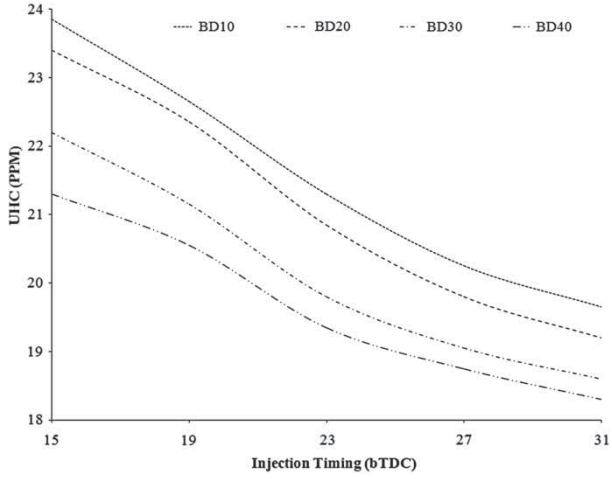

Figure 9. Variation of UBHC at full load with the injection timings.

4.3.3. *UBHC emission*

UBHC emission consists of fuel that is incompletely burnt. Figure 9 depicts the variation of UBHC at full load with the injection timings for all the blends. Advancing injection timing from 23° to 31° bTDC caused reduction of UBHC at full load for all the blends. Advancing the injection caused earlier start of combustion relative to TDC and hence higher cylinder temperatures and thus reduced the HC emission. For retarded injection timings UBHC emissions were higher for all blends. BD40 shows the lowest UBHC emissions for all the injection timings under present study.

4.4. *Prediction of engine performance and exhaust emissions using ANN*

The use of an ANN model is considered as a practical and reliable approach for non-linear problems. The input parameters of the network are blends of polanga with diesel, different injection timings and loads and BSFC, BTE, peak pressure, exhaust gas temperature, NO_x, smoke and UBHC emissions are taken as output parameters. In this study, a computer program has been developed in MATLAB platform to predict BSFC, BTE, peak pressure, exhaust gas temperature, NO_x, smoke and UBHC emissions of the engine. The optimum network structures and statistical parameters of ANN models for different learning algorithms are given in Table 4. It was apparent from Table 4, the prediction performances for both training and testing sets of BSFC, BTE, peak pressure, exhaust gas temperature, NO_x, smoke and UBHC emissions showed that all the approaches provided a quite satisfactory accuracy. Their R values were more than 0.99. The best prediction results were obtained by LM learning algorithm. The LM learning algorithm had the highest speed compared with the other learning algorithms and it reached to optimal solutions with smaller number of neurons in hidden layer.

Table 4. Percentage uncertainties of various instruments.

Instruments	Measuring range	Accuracy	Percentage uncertainties
AVL DiGas 444 Gas Analyser			
HC	0–20,000 ppm vol.	< 200 ppm vol. ± 10 ppm vol. > 200 ppm vol. ± 5%	± 0.3
Nitric oxide (NO)	0–5000 ppm vol.	< 500 ppm vol. ± 50 ppm vol. > 500 ppm vol. ± 10%	± 0.2
AVL-437C Smoke Meter			
Smoke opacity	0–100%	± 1%	± 1
Exhaust gas temperature	0–1250°C	± 1°C	± 0.2
Burette for fuel measurement		± 1 cc	± 1
Pressure transducer	0–100 bar	± 0.01 bar	± 0.1

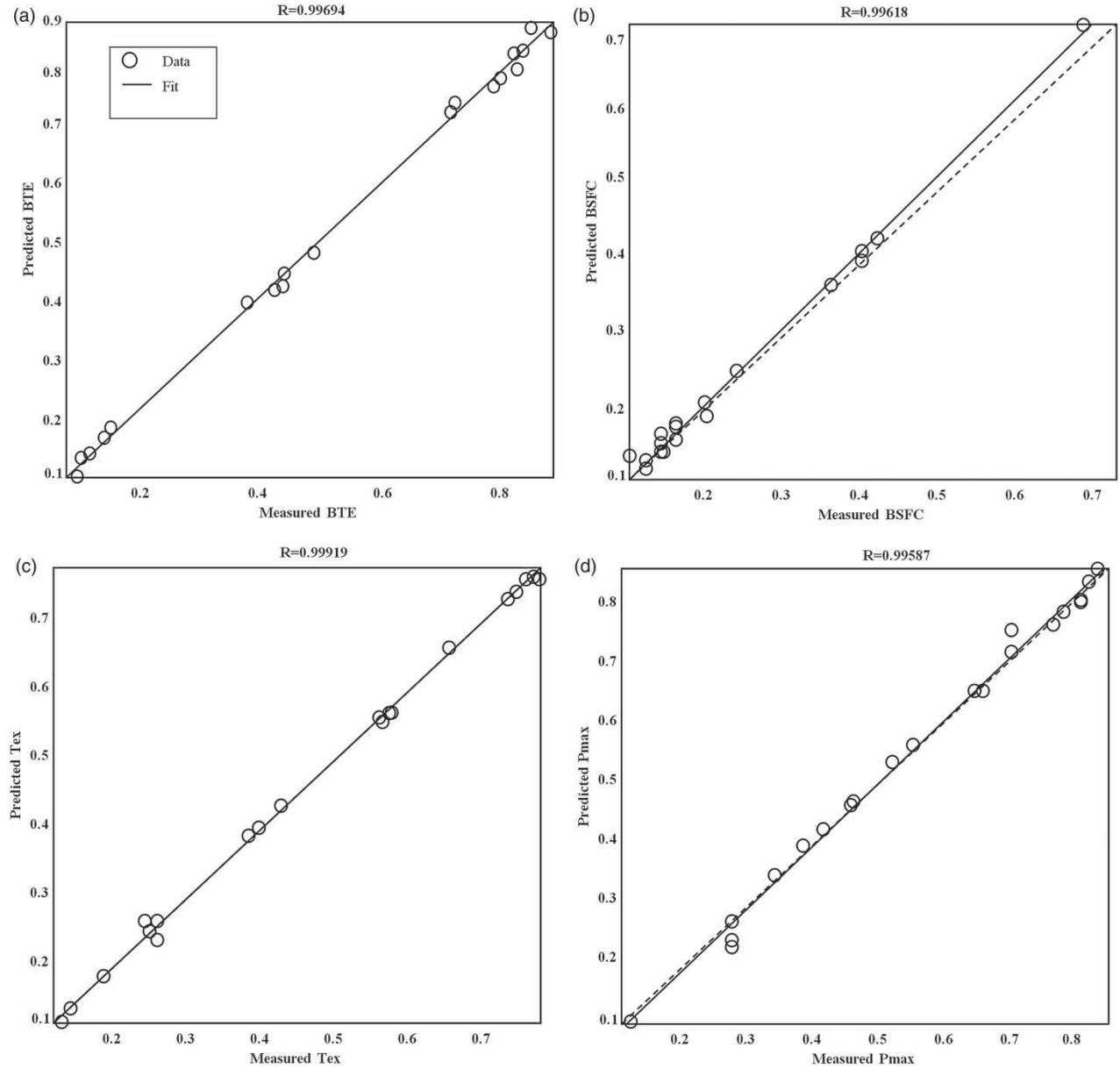

Figure 10. (a) Regression BTE. (b) Regression BSFC. (c) Regression T_{ex}. (d) Regression P_{max}.

Comparisons of the ANN predictions and experimental results for testing sets of output performance parameters are demonstrated in Figure 10. The most striking point here is that the prediction values are very close to the experimental values. As shown in Figure 10, the predictive ability of the network for BTE, BSFC, T_{ex}, P_{max} was found to be satisfactory. This meant that the selection of three input parameters as influencing factors for predictions of engine performance and exhaust emissions provided satisfactory results. The equations of the BTE, BSFC, peak pressure, exhaust gas temperature, NO_x, smoke and UBHC are given in Equations (3)–(9). Also, BTE, peak pressure, exhaust gas temperature, NO_x, smoke and UBHC of the diesel ignition engine which operated with polanga biodiesel can be accurately calculated by these formulae:

$$\mathrm{BTE} = \frac{1}{1 + e^{-\left(\sum_{i=1}^{15} w_{2i}F_i - 0.476\right)}}, \tag{3}$$

Table 5. Weights between input layer and hidden layer for BTE.

i	w_{11}	w_{12}	w_{13}	b_1	w_2
1	− 2.659	− 1.4909	− 7.2222	9.2345	0.49793
2	7.603	3.3924	3.2061	− 4.6459	0.028551
3	1.7752	− 4.0325	− 2.9636	− 3.8798	− 0.17304
4	4.0652	− 4.0882	5.8603	− 3.4281	− 0.00092
5	6.3097	− 5.2133	− 2.3589	− 0.22551	0.047213
6	− 2.0261	0.52794	7.3573	− 4.7258	0.23413
7	1.9165	− 3.034	6.4762	− 1.4443	− 0.10764
8	3.7496	− 5.3014	5.9126	− 0.14011	0.24064
9	0.30894	− 0.13224	− 3.1058	− 2.2361	− 1.7928
10	− 1.7622	2.3105	1.7489	− 0.59645	0.33033
11	2.414	− 6.8167	1.0799	3.0259	0.15199
12	− 2.2804	− 1.9052	1.2801	− 3.0997	− 0.48815
13	− 5.0604	− 8.1969	− 0.5418	− 2.8316	0.02358
14	5.6673	− 2.4137	1.4239	7.5397	0.51033
15	3.2938	− 5.2575	− 2.316	8.0044	− 0.20478

Table 6. Weights between input layer and hidden layer for BSFC.

i	w_{11}	w_{12}	w_{13}	b_1	w_2
1	4.1567	− 6.8758	− 0.62715	− 7.1395	− 0.3121
2	1.2461	− 0.92391	− 5.4306	− 6.2341	1.0329
3	− 3.8544	6.3341	− 0.30276	4.6152	− 0.11413
4	5.6418	2.4093	− 3.6373	− 7.4139	0.34645
5	− 1.1218	2.2638	− 5.7582	0.7759	0.19071
6	− 6.6487	3.6904	2.0569	4.2054	− 0.29359
7	− 3.179	− 7.9002	2.4183	0.53576	1.1479
8	2.8404	9.1259	− 2.7269	− 0.79445	1.1398
9	3.4646	1.2228	5.9325	0.13589	− 0.29822
10	4.6514	0.28008	− 0.71129	4.2639	− 1.0184
11	− 4.3396	7.2366	0.047968	− 4.0393	− 0.07197
12	9.2905	0.1312	0.40156	5.0997	0.84609
13	1.8145	− 0.34113	4.8228	5.2503	− 1.9078
14	− 0.92007	2.4169	6.8491	− 5.5229	− 0.01306
15	4.3419	− 4.516	− 3.9008	6.4368	− 0.15564

$$\mathrm{BSFC} = \frac{1}{1 + e^{-\left(\sum_{i=1}^{15} w_{2i}F_i + 0.83931\right)}}, \tag{4}$$

$$T_{ex} = \frac{1}{1 + e^{-\left(\sum_{i=1}^{15} w_{2i}F_i + 0.83009\right)}}, \tag{5}$$

$$P_{max} = \frac{1}{1 + e^{-\left(\sum_{i=1}^{20} w_{2i}F_i + 0.22691\right)}}, \tag{6}$$

$$\mathrm{NO}x = \frac{1}{1 + e^{-\left(\sum_{i=1}^{20} w_{2i}F_i - 0.49899\right)}}, \tag{7}$$

$$\mathrm{Smoke} = \frac{1}{1 + e^{-\left(\sum_{i=1}^{15} w_{2i}F_i + 2.6321\right)}}, \tag{8}$$

$$\mathrm{UBHC} = \frac{1}{1 + e^{-\left(\sum_{i=1}^{11} w_{2i}F_i + 2.1668\right)}}, \tag{9}$$

Table 7. Weights between input layer and hidden layer for T_{ex}.

i	w_{11}	w_{12}	w_{13}	b_1	w_2
1	− 2.4652	2.9441	− 5.7215	7.755	− 0.07501
2	− 5.291	− 4.1384	− 3.1141	6.6835	− 0.0291
3	− 4.0147	4.7701	− 2.7705	6.7188	− 0.07233
4	− 0.43808	− 3.3905	3.1037	1.3722	0.11408
5	− 0.45786	− 4.5437	0.45357	− 3.082	− 0.88974
6	5.3434	2.4231	− 3.1573	− 3.4994	− 0.02789
7	− 6.6319	1.0581	− 0.81977	1.3066	− 0.1725
8	3.7876	0.074979	− 6.362	− 0.6758	0.027909
9	5.0575	0.77668	0.035999	6.1256	− 1.4504
10	− 0.16347	0.12419	0.80725	− 0.4811	3.7382
11	− 0.34898	− 4.2829	0.63556	− 3.1095	1.0272
12	6.5656	3.2973	0.68616	6.5682	− 0.90005
13	0.54274	3.7039	− 4.3735	− 5.6351	− 0.06222
14	− 5.6862	− 2.2568	− 0.57557	− 6.0582	− 1.5057
15	5.2497	− 0.65505	2.2286	5.8557	0.045858

Table 8. Weights between input layer and hidden layer for P_{max}.

i	w_{11}	w_{12}	w_{13}	b_1	w_2
1	4.0674	− 6.6622	0.18175	− 9.1823	− 0.32554
2	− 2.6438	− 2.1123	6.1137	9.176	0.4758
3	− 3.5482	5.1364	− 3.7255	5.8395	− 0.00046
4	− 6.6239	0.40345	− 1.4243	8.5176	− 1.4155
5	− 5.8759	0.15814	1.0257	5.6111	− 0.26705
6	− 5.8578	− 2.901	− 5.7218	4.4918	− 0.14191
7	0.60466	− 3.9956	7.2408	− 2.6066	− 0.02581
8	− 3.2013	− 0.0126	5.1425	4.8749	0.1594
9	2.6809	7.6185	− 1.7703	− 1.5264	0.13621
10	2.9662	3.2632	− 3.3619	0.59175	− 0.40322
11	− 6.7118	1.9955	3.3735	1.1372	0.28085
12	− 0.81885	5.2898	5.4888	− 1.5393	− 0.24697
13	− 2.4464	3.1157	6.1101	− 1.7371	0.28156
14	5.0377	− 4.0285	− 3.3209	3.544	− 0.17704
15	4.4995	− 0.6158	0.58014	2.2005	2.2618
16	9.0279	− 2.1865	2.1157	4.2704	− 0.76204
17	6.0027	− 5.6314	2.1046	5.1682	− 0.02192
18	− 6.4392	− 5.1445	0.89901	− 7.101	− 0.21539
19	− 3.0931	− 5.4929	4.0787	− 6.8654	0.244
20	− 7.1134	0.98197	3.6646	− 8.0818	0.063698

Table 9. Weights between input layer and hidden layer for NO_x.

i	w_{11}	w_{12}	w_{13}	b_1	w_2
1	− 8.5846	3.0819	3.1	8.2957	0.34036
2	1.5359	0.4366	− 5.9625	− 9.8186	0.54089
3	5.2328	− 0.13306	3.4558	− 9.5163	2.7475
4	3.5419	1.773	− 0.7582	− 6.6261	− 0.25984
5	2.459	− 0.13216	2.2966	− 1.2251	0.93451
6	0.92505	6.452	− 4.2709	− 3.2514	0.013634
7	− 6.1117	3.6304	2.0316	5.2834	− 0.18329
8	− 7.6568	− 1.2626	4.6037	1.8765	0.010837
9	− 6.3861	− 0.13676	4.0037	1.5459	0.39948
10	4.4965	− 3.7435	− 1.0019	− 0.06305	− 0.03127
11	− 3.0729	− 8.4581	− 2.4424	− 0.54576	− 0.01594
12	7.0096	0.1021	− 3.4113	2.9206	− 0.59255
13	− 1.5187	5.1305	7.9937	− 6.0434	− 0.01484
14	3.956	6.1666	− 5.1734	1.1665	0.024616
15	− 4.7473	− 5.5429	7.0341	− 4.489	0.044879
16	− 7.1345	0.036933	0.96463	− 3.115	− 1.0023
17	− 3.5204	0.60142	5.7575	− 5.0108	0.17618
18	1.0973	− 7.5413	− 2.7132	4.1482	− 0.00391
19	− 1.6256	− 7.1912	− 2.4069	− 7.1614	− 0.00695
20	− 3.7432	− 0.85145	− 4.5293	− 7.8385	0.16236

Table 10. Weights between input layer and hidden layer for smoke.

i	w_{11}	w_{12}	w_{13}	b_1	w_2
1	4.0332	− 3.3736	− 5.3406	− 7.7861	− 0.40949
2	0.33131	− 8.5302	4.2813	− 7.1103	− 1.3164
3	− 1.0012	6.4911	− 3.2286	5.195	− 1.5492
4	11.2787	6.5804	− 2.8954	− 5.7425	− 2.1493
5	− 9.1699	− 4.7727	2.858	4.3057	− 2.0181
6	− 0.32597	0.18856	3.045	1.3071	1.2355
7	− 2.3917	− 6.2141	0.2249	1.2614	− 0.60329
8	− 4.5266	3.6809	1.4919	0.47413	0.034515
9	− 7.6513	− 3.5334	1.132	0.32912	0.32639
10	7.1878	3.8044	8.1063	1.9758	0.10416
11	− 8.887	− 0.44626	1.7509	− 0.8346	− 0.21946
12	4.5346	− 4.8819	2.6279	1.744	0.17143
13	− 10.3285	1.1624	0.42189	− 8.1101	0.47927
14	− 2.4782	0.40522	− 6.5778	− 6.3087	− 0.261
15	3.8687	− 7.1257	0.76902	8.125	0.51603

where F_i ($i = 1, 2, 3, \ldots, n$) can be calculated according to Equation (2) in which E_i is the weighted sum of the inputs, and is calculated using

$$E_i = (w_{11} \times \mathrm{IT} + w_{12} \times \mathrm{BD} + w_{13} \times \mathrm{EL} + b_1)i. \quad (10)$$

The data flow was completed with the weights between the layers. The weight values appearing in Equations (3)–(9) are given in Tables 5–11. Here, the effect of the parameters that are at the input layer (injection timing, fuel type and engine load) on the BTE, BSFC, T_{ex}, P_{max}, NO_x, smoke and UBHC can be observed.

Table 11. Weights between input layer and hidden layer for UBHC.

i	w_{11}	w_{12}	w_{13}	b_1	w_2
1	− 0.49679	− 3.5834	4.3696	− 5.0948	− 0.04419
2	− 0.02276	0.10129	1.4006	− 1.6731	− 3.7294
3	− 7.3103	0.036252	− 0.15238	3.4026	− 0.19858
4	6.1033	0.39764	0.043679	− 5.3649	− 0.08389
5	0.021231	4.3231	3.667	− 1.4496	0.66826
6	0.071644	− 8.6226	− 2.8367	− 0.52163	0.55334
7	2.3081	3.399	− 2.0378	3.0818	− 0.0348
8	− 6.5057	− 0.06603	0.30466	− 2.1177	0.17723
9	0.038635	− 7.2043	8.2722	7.0195	− 1.9114
10	0.007006	9.3079	− 6.7053	− 7.7919	− 1.9301
11	− 4.5603	1.5372	2.6846	− 7.2887	0.012742

5. Conclusion

The different polanga blends in the present work can be conveniently used in CI engines as blends with diesel without any engine modifications. Twenty percentage of blend, namely BD20, showed the highest BTE for all the injection timings. It was observed that higher BTE values were obtained at 23° bTDC injection timing, whereas retarding or advancing the injection timing diminished the BTE values. The minimum value of BSFC was obtained for BD20 at the best injection timing of 23° bTDC. BD10 showed the lowest values of exhaust temperature at all the injection timings. An ANN was developed and trained with the experimental data of the present work. The result showed that the training algorithm of back-propagation was sufficient enough in predicting BSFC, BTE, peak pressure, exhaust gas temperature and exhaust gas components for different injection timings and different fuel blends ratios. It has also been observed that R values were very close to one for BTE, BSFC, peak pressure, exhaust gas temperature, NO_x, smoke and UBHC. Analysis of the experimental data by the ANN revealed that there was good correlation between the predicted data resulted from the ANN and measured ones. The developed model thus reduces the experimental efforts and hence can serve as an effective tool for predicting the performance of the engine and emission characteristics under various operating conditions with different biodiesel blends.

Acknowledgement

The authors are highly thankful to Dr Harshdeep Sharma, School of Mechanical Engineering, Galgotias University, Greater Noida (India) for his valuable advice and support throughout this work.

Disclosure statement

No potential conflict of interest was reported by the authors.

References

Ahmadi, Mohammad H., S. S. Ghare Aghaj, and A. Nazeri. 2013a. “Prediction of Power in Solar Stirling Heat Engine by

Using Neural Network Based on Hybrid Genetic Algorithm and Particle Swarm Optimization." *Neural Computing and Applications* 22 (6): 1141–1150.

Ahmadi, Mohammad H., Mehdi Mehrpooya, and Nima Khalilpoor. 2014a. "Artificial Neural Networks Modelling of the Performance Parameters of the Stirling Engine." *International Journal of Ambient Energy*. doi:10.1080/01430750.2014.964370

Ahmadi, Mohammad H., A. H. Mohammadi, and S. Dehghani. 2013b. "Evaluation of the Maximized Power of a Regenerative Endoreversible Stirling Cycle Using the Thermodynamic Analysis." *Energy Conversion and Management* 76: 561–570.

Ahmadi, Mohammad H., A. H. Mohammadi, S. Dehghani, M. Feidt, and M. A. Barranco-Jiménez. 2013. "Optimal Design of a Solar Driven Heat Engine Based on Thermal and Thermoeconomic Criteria." *Energy Conversion and Management* 75: 635–642.

Ahmadi, Mohammad H., Amir H. Mohammadi, and S. Mohsen Pourkiaei. 2014b. "Optimisation of the Thermodynamic Performance of the Stirling Engine." *International Journal of Ambient Energy*. doi:10.1080/01430750.2014.907211

Ahmadi, Mohammad H., H. Sayyaadi, and A. H. Mohammadi. 2013c. "Application of the Multi-objective Optimization Method for Designing a Powered Stirling Heat Engine: Design with Maximized Power. Thermal Efficiency and Minimized Pressure Loss." *Renew Energy* 60: 313–322.

Baiju, B., M. K. Naik, and L. M. Das. 2009. "A Comparative Evaluation of Compression Ignition Engine Characteristics Using Methyl and Ethyl Esters of Karanja Oil." *Renewable Energy* 34: 1616–1621.

Canakci, M., and J. V. Gerpen. 2003. "Comparison of Engine Performance and Emissions for Petroleum Diesel Fuel, Yellow-Grease Biodiesel and Soybean-Oil Biodiesel." *Transactions of the ASAE* 46 (4): 937–944.

Canakci, M., A. N. Ozsezen, E. Arcaklioglu, and A. Erdil. 2009. "Prediction of Performance and Exhaust Emissions of a Diesel Engine Fuelled with Biodiesel Produced from Waste Frying Palm Oil." *Expert Systems with Applications* 36: 9268–9280.

Çay, Y., I. Korkmaz, A. Çiçek, and F. Kara. 2013. "Prediction of Engine Performance and Exhaust Emissions for Gasoline and Methanol Using Artificial Neural Network." *Energy* 50: 177–186.

Ghobadian, B., H. Rahimi, A. M. Nikbakht, G. Najafi, and T. F. Yusaf. 2009. "Diesel Engine Performance and Exhaust Emission Analysis Using Waste Cooking Biodiesel Fuel with an Artificial Neural Network." *Renewable Energy* 34 (4): 976–982.

Ismail, H. M., N. H. Kiat, C. W. Queck, and S. Gan. 2012. "Artificial Neural Networks Modelling of Engine-Out Responses for a Light-Duty Diesel Engine Fuelled with Biodiesel Blends." *Applied Energy* 92: 769–777.

Ramadhas, A. S., S. Jayaraj, and C. Muraleedharan. 2005. "Biodiesel Production from High FFA Rubber Seed Oil." *Fuel* 84: 335–340.

Sahoo, P. K., L. M. Das, M. K. G. Babu, P. Arora, V. P. Singh, N. R. Kumar, and T. S. Varyani. 2009. "Comparative Evaluation of Performance and Emission Characteristics of Jatropha, Karanja and Polanga Based Biodiesel as Fuel in a Tractor Engine." *Fuel* 88: 1698–1707.

Sahoo, P. K., L. M. Das, M. K. G. Babu, and S. N. Naik. 2007. "Biodiesel Development from High Acid Value Polanga Seed Oil and Performance Evaluation in a CI Engine." *Fuel* 86: 448–454.

Shivakumar, P.Srinivasa Pai, and B. R.Shrinivasa Rao. 2011. "Artificial Neural Network Based Prediction of Performance and Emission Characteristics of a Variable Compression Ratio CI Engine Using WCO as a Biodiesel at Different Injection Timings." *Applied Energy* 88: 2344–2354.

Toghyani, Somayeh, Mohammad H. Ahmadi, Alibakhsh Kasaeian, and Amir H. Mohammadi. 2015. "Artificial Neural Network, ANN-PSO and ANN-ICA for Modelling the Stirling Engine." *International Journal of Ambient Energy*. doi:10.1080/01430750.2014.986289

Toghyani, Somayeh, A. Kasaeian, and M. H. Ahmadi. 2014. "Multiobjective Optimization of Stirling Engine Using Non-ideal Adiabatic Method." *Energy Conversion and Management* 80: 54–62.

Yusaf, T. F., D. R. Buttsworth, K. H. Saleh, andB. F. Yousif. 2010. "CNG-Diesel Engine Performance and Exhaust Emission Analysis with the Aid of Artificial Neural Network." *Applied Energy* 87: 1661–1669.